ICARUS 80, 211–219 (1989)

NOTES

On the Obliquity and Tidal Heating of Triton

DAVID G. JANKOWSKI, CHRISTOPHER F. CHYBA, AND PHILIP D. NICHOLSON

Center for Radiophysics and Space Research, Cornell University, Ithaca, New York 14853

Received March 8, 1989; revised April 11, 1989

Alone of all the major Solar System satellites, Triton may have an obliquity near 100°. Such an obliquity could result in significant tidal heating of the satellite and will eventually lead to damping of its orbital inclination to 180°. © 1989 Academic Press, Inc.

INTRODUCTION

Triton is a most unusual satellite in several respects. Moving on a nearly circular orbit at 14 Neptune radii with an inclination of 159°, Triton fits neither into the category of "regular" satellites (nearly circular, low inclination, prograde orbits) nor into that of the "irregular" satellites (distant, often retrograde, highly elongated, and highly inclined orbits) (Goldreich 1966). Its unusual orbital characteristics have led to the suggestion that Triton did not accrete in orbit about Neptune, but is instead a captured body (McKinnon 1984). Here we explore the possibility that Triton is unusual in yet another way: its rotational state.

In introducing the subject of satellite rotational states it is both useful and historically relevant to consider the Moon. In 1693, G. D. Cassini published three laws describing lunar motion. He noted that (1) the rotation of the Moon is synchronous with its orbital motion, (2) the lunar spin axis maintains a constant inclination of ~1.5° to the ecliptic plane, and (3) the lunar spin axis and orbit normal remain coplanar with one another, and with the ecliptic normal, during their mutual precessional motion (Colombo 1966).

Due to gravitational torques exerted by the Sun, the lunar orbit plane currently regresses with a period of 18.6 years. The lunar orbit normal thus sweeps out a cone, maintaining a constant inclination of 5.2° from the normal to the ecliptic plane. In satisfying Cassini's third law, the Moon's spin axis also regresses about the normal to the ecliptic plane with the same 18.6-year period. This latter precession is caused by torques exerted by the Earth on the nonspherical figure of the Moon. Such coprecession is only possible for values of the lunar obliquity, θ (measured from the orbit normal), which satisfy the expression (Peale 1969)

$$(\tfrac{3}{2})n\gamma \sin\theta \cos\theta + (\tfrac{3}{8})n\beta \sin\theta(1 - \cos\theta) - \dot{\Omega} \sin(\theta - I) = 0. \quad (1)$$

Here, n is the Moon's orbital mean motion, $-\dot{\Omega}$ is the orbital precession rate, I is the orbital inclination, $\gamma = (C - A)/C$, and $\beta = (B - A)/C$. $A < B < C$ are the lunar principal moments of inertia. Solutions to Eq. (1) are called Cassini states. For the Moon, $\theta = 6.7°$, measured from the orbit normal toward the ecliptic normal, so that the spin axis and orbit normal are located on opposite sides of the ecliptic normal. Equation (1) can be generalized to any spin-locked satellite undergoing orbital precession at a uniform rate. All regular satellites fall into this category and are expected to occupy the appropriate Cassini states (Peale 1977).

0019-1035/89 $3.00

CASSINI STATES

In general, the motion of a satellite's spin axis can best be visualized by examining the Hamiltonian of the system. In a coordinate system coprecessing with the orbit plane, the Hamiltonian is a constant of the motion, and its level curves thus prescribe the allowed spin axis trajectories (Colombo 1966). Figure 1a shows the projection of the unit sphere on the rotating plane containing the orbit normal (the Z axis) and perpendicular to the ascending node of the orbit on the invariable plane (the X axis, out of the page) for parameters appropriate to Triton.[1]

In this coordinate system, the precession trajectories of the spin vector follow the intersection of the parabolic cylinder

$$(Z - K_1)^2 = K_2(Y - K_3) \qquad (2)$$

with the unit sphere, where two of the three constants are given by (Peale 1977, Eqs. (25)–(28))

$$K_1 = \frac{(\cos I - 2S)}{2(R + S)} \qquad (3)$$

$$K_2 = \frac{\sin I}{(R + S)} \qquad (4)$$

and where, for a circular orbit,

$$R = \frac{3n^2(\gamma - \beta/2)}{4\dot{\Omega}\dot{\psi}} \qquad (5)$$

$$S = \frac{3n\beta}{16\dot{\Omega}}. \qquad (6)$$

$\dot{\psi}$ and $\dot{\Omega}$ are the satellite spin angular velocity and magnitude of the orbital precession rate, respectively. Equation (6) holds only for synchronous rotation; for nonsynchronous rotation, $S = 0$. The third constant, K_3, is determined by the Hamiltonian of the system in the rotating coordinate frame. Figure 1a shows some representative precessional trajectories for Triton's spin axis (solid lines). The different parabolas are obtained by varying the parameter K_3, which slides the parabolic cylinder along the Y axis.

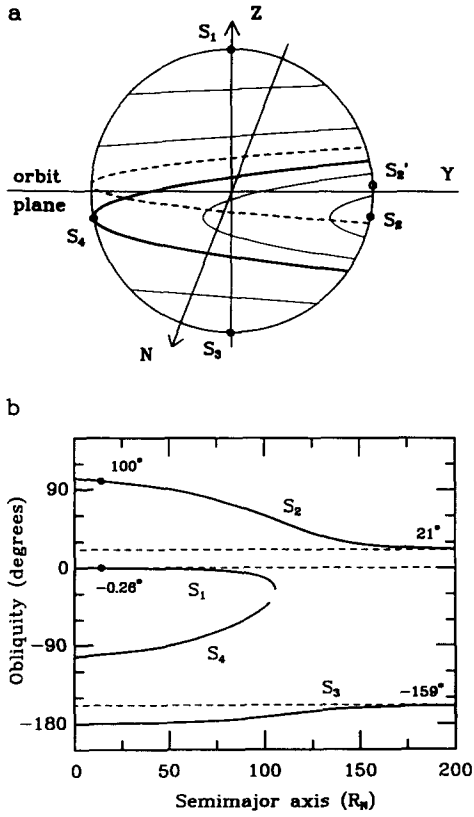

FIG. 1. (a) Precession trajectories of Triton's spin vector on the unit sphere. The Z axis is Triton's orbit normal, and N denotes the normal to the Neptune–Triton invariable plane, about which Triton's orbit precesses. The solid circles mark the locations of the four Cassini states. The dotted line shows the critical parabola (see text) immediately prior to spin-locking. The heavy solid line shows the critical parabola after spin-locking. (b) Obliquities of the four Cassini states as a function of Triton's orbital semimajor axis for the present inclination of 159° and zero eccentricity. The solid circles indicate the two possible obliquities which are stable in the presence of tidal torques.

[1] For Triton, the invariable plane is defined by the total angular momentum vector of the Neptune-Triton system, and is located close to the planet's equatorial plane (Harris 1984). For our purposes, however, it is simpler to abandon a Neptunocentric viewpoint and to treat Triton's orbit as prograde, with an inclination of 21°, regressing about the (inverted) invariable plane normal. This is entirely equivalent to the more conventional viewpoint, but emphasizes the correspondence between the Cassini states of Triton and those of prograde satellites.

Cassini states correspond to extrema of the Hamiltonian and are thus found at those locations where parabolic cylinders are tangent to the unit sphere. Triton's current possible Cassini states are shown in Fig. 1a by the four solid circles labeled S_1 through S_4. From the diagram, it is evident that libration is possible about any of states S_1 through S_3, while state S_4 is dynamically unstable.

In general, a satellite will possess either two or four possible Cassini states, depending upon the values of $n\gamma/\dot{\Omega}$ and $n\beta/\dot{\Omega}$. Decreasing these ratios increases the coefficients K_1 and K_2, thus shifting the corresponding parabolic cylinders up the Z axis and causing them to increase in width. As K_1 nears unity, a point is reached where only two parabolic cylinders are tangent to the sphere. At this point, states S_1 and S_4 merge, and then cease to exist for larger values of K_1. The Moon currently falls into this category and is observed to lie in Cassini state 2.

Variations in the semimajor axis due, for example, to tidal evolution, change both the spin and orbital precession rates. Figure 1b shows the locations of Triton's Cassini states as a function of semimajor axis, a, for Triton's current eccentricity (zero) and inclination. (Because of its retrograde orbit, Triton must currently be evolving toward Neptune under the influence of tides it raises on the planet, though the rate of this evolution is probably much less than that estimated by McCord (1966; also see Harris 1984). Tidal evolution is expected, however, to have produced only modest changes in inclination, though the same cannot necessarily be said for the eccentricity (Chyba *et al.* 1989).) As a is increased, the ratios $n\gamma/\dot{\Omega}$ and $n\beta/\dot{\Omega}$ decrease until, at about 105 R_N, Cassini states 1 and 4 disappear. Beyond ~75 R_N, $\dot{\Omega}$ is dominated by solar perturbations, rather than by Neptune's oblateness. A similar diagram was constructed for the Moon by Ward (1975a), from which he deduced that the Moon probably resided in Cassini state 1 until the tidal expansion of its orbit caused that state to disappear at ~35 R_E.

TIDAL DESPINNING

In the presence of tidal dissipation, the same torques that despin a satellite act to drive its spin vector toward a Cassini state (Peale 1974, Ward 1975b). However, not all Cassini states are possible end points of tidal evolution. Although the spin vector may librate about state 3, the influence of tides renders this state unstable over longer time scales (Peale 1974). (Core–mantle interactions and/or atmospheric thermal tides have been proposed to maintain Venus's retrograde spin orientation near state 3 (Goldreich and Peale 1970), but such mechanisms seem unlikely to apply to satellites and are not considered further here.) This leaves Cassini states 1 and 2 as the only possible end points of tidal evolution. The time scale for collapse to a Cassini state is comparable to a satellite's despinning time scale (Peale 1974). Thus all spin-locked satellites should currently lie very close to one of these two Cassini states.

Ground-based observations of Triton have tentatively found a synchronous rotational state (Franz 1981) consistent with predicted despinning times (~10^4 years for Q_T = 100; Peale 1977), indicating that Triton is almost certainly rotating synchronously. The solid circles in Fig. 1b show the two possible current spin states for Triton: S_1 at an obliquity of −0.26° and S_2 at 100°. Beyond ~100 R_N, only state 2 is stable, and Triton's spin axis would have been located close to the normal to its invariable plane (= Neptune's orbit plane, at this distance). Inward tidal evolution would then have resulted in Triton's present obliquity being ~100°. However, despinning time scales for Triton beyond 100 R_N are longer than the age of the Solar System, unless the orbit is highly eccentric (in which case states 1 and 4 survive out to greater distances.) Thus if Triton has evolved in from some great distance, it is unlikely to have collapsed into any Cassini state until well in-

side of 100 R_N, where both states 1 and 2 are possible end points.

The mass and radius of Triton are poorly known. We adopt here a radius of 1750 km, consistent with radiometric measurements (Morrison *et al.* 1982, Lebofsky *et al.* 1982). However, this value when combined with the best mass determinations (Alden 1943, Duncombe *et al.* 1974) yields a prohibitively high density (~6 g cm^{-3}). We therefore assume a more realistic density for a large icy satellite of $\rho = 2.0$ g cm^{-3}, corresponding to a mass ratio $M_T/M_N = 0.00044$. If $\rho = 3.0$ g cm^{-3}, the Cassini state obliquities become $S_1 = -0.^\circ40$ and $S_2 = 98^\circ$, while if $\rho = 1.3$ g cm^{-3}, we have $S_1 = -0.^\circ17$ and $S_2 = 101^\circ$.

COMPARISON OF TRITON WITH OTHER SATELLITES

In Table I we compare the two possible spin orientations of Triton with the theoretical Cassini obliquities for the principal regular satellites; for completeness, we also give the inclinations and orbital precession rates used in the calculations. Hydrostatic moment differences were calculated separately for each Cassini state (subscripts 1

TABLE I

HYDROSTATIC MOMENT DIFFERENCES AND STABLE CASSINI STATE OBLIQUITIES

Satellite	I^a (deg)	$\dot{\Omega}^b$ (deg year^{-1})	Moment differences ($\times 10^{-3}$)				Obliquities (deg)		Λ^c
			γ_1	β_1	γ_2	β_2	S_1	S_2	
Moon[d]	5.15	19.3	—	—	0.63	0.23	—	6.7	—
Io	0.040	48.6	8.49	6.37	1.36	1.66	0.00	89.	5.1
Europa	0.470	12.0	2.53	1.90	0.513	0.637	0.04	81.	1.3
Ganymede	0.195	2.63	0.953	0.715	0.212	0.260	0.02	78.	2.0
Callisto	0.281	0.643	0.183	0.137	0.0826	0.0816	0.12	57.	4.4
Mimas	1.53	365.	90.7	68.0	13.0	12.6	0.03	98.	1.6
Enceladus	0.02	153.	39.1	29.3	5.63	5.93	0.00	96.	11.
Tethys	1.09	72.2	21.6	16.2	3.15	3.46	0.04	94.	1.3
Dione	0.02	31.0	9.03	6.77	1.42	1.71	0.00	90.	7.6
Rhea	0.35	10.1	3.46	2.60	0.615	0.768	0.03	85.	1.5
Titan	0.33	0.50	0.198	0.149	0.0698	0.0752	0.08	65.	2.5
Iapetus[e]	7.52	0.12	—	—	0.020	0.010	—	13.	—
Iapetus[f]	7.52	0.12	0.63	0.23	0.63	0.23	0.62	91.	—
Miranda	4.22	20.4	41.0	30.8	6.00	4.74	0.02	102.	2.5
Ariel	0.31	6.07	9.63	7.22	1.39	1.17	0.00	101.	5.9
Umbriel	0.36	2.94	3.66	2.74	0.523	0.492	0.01	99.	3.6
Titania	0.14	1.23	0.786	0.589	0.143	0.178	0.01	84.	2.3
Oberon	0.10	0.928	0.337	0.253	0.112	0.123	0.02	67.	4.4
Triton	159.	−0.578	1.37	1.03	0.196	0.175	0.26	100.	0.6

[a] Inclinations and satellite physical parameters are from Burns (1986).

[b] Orbital precession rates for the Jovian and Saturnian satellites (except for Iapetus) and for Triton are from the Astronomical Almanac for the year 1989, U.S. Government Printing Office, Washington, DC. The value for Iapetus is from Peale (1977). The precession rates of the Uranian satellites all vary considerably with time due to mutual secular perturbations (Dermott and Nicholson 1986). The rates shown for these satellites are mean values calculated using masses and Uranus gravity parameters from Tyler *et al.* (1986).

[c] $\Lambda = |K_1^{(2)} - K_1^{(0)}|/\sqrt{2K_2^{(2)}\cos(K_1^{(2)})}$, for small $K_1^{(2)}$, where the superscripts 0 and 2 refer to values immediately before and after synchronization in Cassini state 2, respectively.

[d] Lunar moment differences are from Peale (1977).

[e] Assuming hydrostatic moment differences.

[f] Assuming lunar moment differences.

and 2 refer to Cassini states 1 and 2, respectively). For the hydrostatic moment differences for a synchronously rotating satellite with nonzero obliquity, we find

$$\gamma(\theta) = (5q/32)(5 + 6\cos\theta + 21\cos^2\theta) \quad (7)$$

$$\beta(\theta) = (15q/16)(1 + \cos\theta)^2, \quad (8)$$

where $q = (M_P/M_S)(R_S/a)^3$, M_P is the primary mass, and M_S, R_S, and a are the satellite mass, radius, and semimajor axis, respectively. Equations (1), (7), and (8) were solved self-consistently for the obliquities and moment differences listed in Table I.

Note that two entities are shown for Iapetus. If Iapetus possessed close to hydrostatic moments, it would lie in state 2 (Ward 1975b). If somewhat large lunar-like moment differences are assumed, however, Cassini state 1 will also exist (Peale 1977). Voyager images revealed that Iapetus has an obliquity very close to 0° (Davies and Katayama 1984), indicating that Iapetus's moment differences are larger than hydrostatic.

Observations thus far have shown that all spin-locked satellites appear to have their spin axes oriented approximately normal to their orbit planes. The obliquities listed in Table I indicate that all of these satellites, with the exception of the Moon, must lie in state 1. In order to understand the prevalence of satellites in state 1, and to assess the likelihood of Triton's occupying state 2, it is necessary to examine spin axis evolution prior to collapse into a Cassini state.

CHOOSING A CASSINI STATE

In Fig. 1a the precession trajectory passing through Cassini state 4, hereafter called the "critical parabola," is of fundamental importance in determining which Cassini state is selected as an end point. Initial spin orientations above the critical parabola are driven by tides to state 1, while initial spin orientations inside of the critical parabola are driven to state 2. Initial spin orientations below the critical parabola are driven by tides up to and inside of the critical parabola, eventually evolving to state 2 (Peale 1974). Thus if a satellite's spin orientation is ever inside or below its critical parabola, its spin vector will evolve to Cassini state 2.

Since most satellites have small K_1 values (see Peale 1977), their critical parabolas are narrow and centered very close to the Y axis in Fig. 1a If these satellites' primordial obliquities were larger than about 90°, their spin axes would have evolved to state 2. Since most satellites' rotational states have been significantly altered by tides, our knowledge of their primordial spin states is poor. If we assume random orientations for the primordial spin axes, then roughly one-half of the satellites would have initial obliquities greater than 90°. If satellite formation results in initial spin states similar to those resulting from planetary formation, then perhaps one-quarter of the satellites would have initial obliquities greater than 90°. For captured satellites, random spin axis orientations again seem probable. In any event, it seems highly unlikely that *no* regular satellites formed with primordial obliquities larger than 90°. We are thus led to examaine the durability of Cassini state 2 as an end point of tidal evolution in more detail.

The width of the critical parabola, determined by the parameter K_2, is an important measure of the stability of Cassini state 2. The range of obliquities enclosed by this parabola in the Y–Z plane is given by $\sin^{-1}(2\sqrt{2K_2\cos(K_1)})$, where K_1 is assumed small. Triton's critical parabola encloses about 50° (see Fig. 1a). However, $K_2 \propto \sin I$, so that for most regular satellites the critical parabola is much narrower.

For satellites with sufficiently narrow critical parabolas, Cassini state 2 is not a likely end point because of the spin-locking event itself. When a satellite attains synchronous rotation, its critical parabola undergoes two "shifts." An instantaneous shift is caused as the satellite's orientation becomes fixed relative to the planet and the parameter S becomes nonzero (Peale 1974).

The size of this shift is determined by the satellite's β value immediately prior to spin-locking. A second shift is caused by the adjustments in the satellite's γ and β values as it relaxes from an oblate spheroid to a tidally distorted triaxial ellipsoid. This second shift is not instantaneous, but occurs over a time dependent upon the satellite's physical parameters (Darwin 1879). Both of these effects decrease K_1, although if the relaxation time is long compared with the precessional period of the satellite's spin axis about the Cassini state, then the spin axis may adiabatically follow the second shift. Thus, while the obliquity of the satellite remains essentially fixed, its critical parabola shifts *down* the Z axis. The dashed line in Fig. 1a shows the critical parabola for Triton immediately prior to spin-locking, where we have assumed for simplicity purely hydrostatic moments and Triton's current orbital semimajor axis.

For a satellite to evolve to Cassini state 2, it must not only be driven toward state 2 by tides prior to synchronization, but also afterward. In other words, the spin vector after spin-locking, which should be very close to the old (presynchronization) Cassini state 2 point, must also lie inside of the new (postsynchronization) critical parabola. In Fig. 1a, Triton's old Cassini state 2 location is marked by the open circle. It is clear from the figure that Triton's new critical parabola is broad enough to contain the old Cassini state 2 location after the spin-locking event. If Triton's preexisting β were less than the hydrostatic value assumed here, this conclusion is strengthened.

Although Cassini state 2 is not rendered unstable during the spin-locking event for Triton, such is the case for the other satellites. We have investigated the stability of state 2 for each of the satellites in Table I. The column marked Λ shows the ratio of the shift in the K_1 parameter due to spin-locking to the half-width of the new critical parabola, assuming hydrostatic moments throughout. For $\Lambda > 1$, the old Cassini state 2 position (the location of the spin vector) is left *above* the new critical parabola after spin-locking. Tidal forces then drive the spin to state 1. Due to its large inclination, Triton is the only satellite with $\Lambda < 1$ (this is true for densities of 1.3 and 3.0 g cm^{-3} also) and, hence, is the only satellite for which Cassini state 2 is not rendered unstable during synchronization. (In a few cases where Λ is close to unity, this conclusion might be altered by the presence of preexisting moments very different from the hydrostatic values assumed here or by allowing for tidal evolution of the satellite's semimajor axis since synchronization.)

Recent work by Wisdom (1987) indicates that irregularly shaped satellites must tumble chaotically immediately prior to synchronization. It is unclear if this holds for larger, more regularly shaped satellites. For satellites passing through such a chaotic state, Cassini state 2 might not be rendered unstable by synchronization. However, the narrow width of the critical parabola for most satellites suggests that subsequent escape from state 2 due either to impactors or to orbital perturbations is likely (Peale 1974).

HEATING DUE TO OBLIQUITY TIDES

Although tidal heating is generally associated with spin-locked satellites on eccentric orbits, a satellite with a large obliquity can undergo substantial heating due to obliquity tides, even on a circular orbit. In such a case, the satellite's elastic tidal bulge will sweep above and below its equator, resulting in frictional heating of the satellite's interior. In Cassini state 2, with an obliquity near 90°, the tidal bulge moves almost from one pole to the other, crossing the equator twice each orbit (see Fig. 2).

A tidal heating model which accounts for both the eccentricity and obliquity effects has been developed by Peale and Cassen (1978). Applying their model of an incompressible homogeneous satellite with zero eccentricity but nonzero obliquity, and assuming a frequency-independent Q, we find

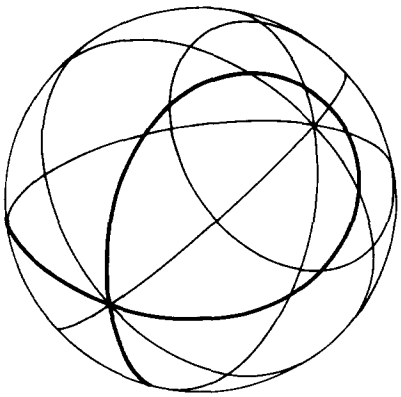

FIG. 2. The path of the sub-Neptune point on the surface of Triton over one orbit, assuming a Cassini state 2 orientation. The elastic tidal bulge will follow this path, lagging the sub-Neptune point in time due to the anelasticity of the satellite. For a Cassini state 1 orientation, the sub-Neptune point would remain essentially at one point, located on Triton's equator.

for the energy dissipation rate

$$dE/dt = (\tfrac{21}{2})(k_2/1 + k_2)(R_S^5 n^5/GQ) \sin^2 \theta \quad (\theta \approx 0°) \quad (9a)$$

$$dE/dt = (\tfrac{15}{8})(k_2/1 + k_2)(R_S^5 n^5/GQ) \quad (\theta \approx 90°), \quad (9b)$$

where Q is the tidal dissipation factor (see Goldreich and Soter 1966), and k_2 is the second-order Love number (see Munk and MacDonald 1960). The latter is given by

$$k_2 = (\tfrac{3}{2})/(1 + 19\mu/2\rho g R_S), \quad (10)$$

where μ is the satellite's modulus of rigidity and g is its surface gravity. As Triton's radius and bulk composition are unknown, we have calculated heating rates for both a primarily icy Triton ($\rho = 1.3$ g cm^{-3}, $\mu = 4 \times 10^{10}$ dyn cm^{-2}; Proctor 1966) and a mostly silicate Triton ($\rho = 3.0$ g cm^{-3}, $\mu = 3 \times 10^{11}$ dyn cm^{-2}; Bullen 1981), for radii between 1500 and 2000 km. For a Q of 100, we find the Cassini state 2 heating rates

$$(dE/dt)_{icy} = (2.5 - 18) \times 10^{20} \text{ erg sec}^{-1} \quad (11a)$$

$$(dE/dt)_{sil} = (1.0 - 6.8) \times 10^{20} \text{ erg sec}^{-1} \quad (11b)$$

where the larger heating rates refer to the larger radius. The corresponding Cassini state 1 heating rates are lower by roughly five orders of magnitude, and thus quite negligible.

The Cassini state 2 heating rates are much higher than the maximum plausible radiogenic heating rates (for a large, primarily silicate Triton, $(dE/dt)_{rad} = 5.0 \times 10^{18}$ erg sec^{-1}). In fact, they exceed the tidal heating rate calculated for Io using the same model (Peale *et al.* 1979). The largest heating rate in (11a) is capable of heating the surface of Triton isothermally up to ~90 K. This is clearly inconsistent with observations of Triton (Morrison *et al.* 1982). However, the lower heating rates could escape detection, particularly if the heat is preferentially radiated in a few localized regions, as is the case for Io.

Clearly such heating would have important consequences for the present state of Triton's interior and surface, as well as the satellite's orbital evolution (Chyba *et al.* 1989). The only satellite known to be undergoing significant tidal heating is Io. One must be careful in drawing analogies between a tidally heated Triton and Io, however, due to their almost certainly very different bulk compositions and mechanisms of tidal heating. However, it is expected that such violent heating would result in widespread volcanism and outgassing.

CONCLUSIONS

What is the probability that Triton is now, or was at one time, in Cassini state 2? We have argued that Triton's substantial orbital inclination results in an unusually broad region of stability for obliquities near 100°, sufficient to ensure the preservation of state 2 during the spin-locking process itself, and in the presence of modest impact-induced displacements in the spin axis. This is in contrast to the situation for most (perhaps all) other tidally despun satellites.

If Triton does have such a large obliquity, it could presently be undergoing sig-

nificant heating due to obliquity tides. The results of such heating should be evident during the August 1989 *Voyager* flyby.

Ironically, the strongest argument against Triton's current residence in state 2 follows from the substantial orbital inclination and the resulting energy dissipation due to obliquity tides. This energy loss, with no accompanying change in the component of Triton's total angular momentum perpendicular to the invariable plane, will inevitably lead to a damping of the inclination to 180° (Chyba *et al.* 1989). For the heating rates calculated above in state 2, the damping time scale is 2×10^7 to 2×10^8 years. Unless we are privileged to live at a very special time in Triton's history, or unless $Q_T \geq 10^3$, it therefore seems unlikely, if not impossible, that Triton's obliquity is presently ~100°. Should Triton indeed be found to have an obliquity ~100°, then we can set a plausible lower limit on its Q, which may well be applicable to other icy satellites.

If Triton had occupied state 2 at an earlier period in its history, and Q_T were not large, then obliquity tides should have rapidly damped its inclination to 180°, at which point the critical parabola shrinks to zero width and state 2 becomes unstable. The obliquity would then damp to zero.

ACKNOWLEDGMENTS

We thank Joe Burns, Peter Goldreich, Stan Peale, and Charles Yoder for helpful discussions. We also thank Anthony Dobrovolskis and an anonymous referee for their reviews of the manuscript. This work was supported in part by NASA Grants NGR 33-010-220 and NAGW-544, and the Planetary Geology and Geophysics Program.

REFERENCES

ALDEN, H. L. 1943. Observations of the satellite of Neptune. *Astron. J.* **50,** 110–111.

BULLEN, K. E. 1981. *The Earth's Density*. Halsted, New York.

BURNS, J. A. 1966. Some background about satellites. In *Satellites* (J. A. Burns and M. S. Matthews, Eds.), pp. 1–38. Univ. of Arizona Press, Tucson.

CASSINI, G. D. 1693. *Traité de l'origine et de progrès de l'astronomie*. Paris.

CHYBA, C. F., D. G. JANKOWSKI, AND P. D. NICHOLSON. 1989. Tidal Evolution in the Neptune–Triton System. *Astronom. and Astrophys.* In press.

COLOMBO, G. 1966. Cassini's second and third laws. *Astron. J.* **71,** 891–896.

DARWIN, G. H. 1879. On the bodily tides of viscous and semi-elastic spheroids, and on the ocean tides upon a yielding nucleus. *Philos. Trans. R. Soc. London Ser. A* **170,** 1–35.

DAVIES, M. E., AND F. Y. KATAYAMA 1984. The control network of Iapetus. *Icarus* **59,** 199–204.

DERMOTT, S. F., AND P. D. NICHOLSON 1986. Masses of the satellites of Uranus. *Nature (London)* **319,** 115–120.

DUNCOMBE, R. L., W. J. KLEPCZYNSKI, AND P. K. SEIDELMANN 1974. The masses of the planets, satellites, and asteroids. *Fundam. Cos. Phys.* **1,** 119–165.

FRANZ, O. G. 1981. UBV photometry of Triton. *Icarus* **45,** 602–606.

GOLDREICH, P. 1966. History of the lunar orbit. *Rev. Geophys.* **4,** 411–439.

GOLDREICH, P., AND S. J. PEALE 1970. The obliquity of Venus. *Astron. J.* **75,** 273–283.

GOLDREICH, P., AND S. SOTER 1966. Q in the Solar System. *Icarus* **5,** 375–389.

HARRIS, A. W. 1984. Physical properties of Neptune and Triton inferred from the orbit of Triton. In *Uranus and Neptune*, NASA CP-2330, pp. 357–376.

LEBOFSKY, L. A., G. H. RIEKE, AND M. J. LEBOFSKY 1982. The radii and albedos of Triton and Pluto. *Bull. Amer. Astron. Soc.* **14,** 766.

MCCORD, T. B. 1966. Dynamical evolution of the Neptunian system. *Astron. J* **71,** 585–590.

MCKINNON, W. B. 1984. On the origin of Triton and Pluto. *Nature (London)* **311,** 355–358.

MORRISON, D., D. P. CRUIKSHANK, AND R. H. BROWN 1982. Diameters of Triton and Pluto. *Nature (London)* **300,** 425–426.

MUNK, W. H., AND G. J. F. MACDONALD 1960. *The Rotation of the Earth*. Cambridge Univ. Press, London.

PEALE, S. J. 1969. Generalized Cassini's laws. *Astron. J.* **74,** 483–489.

PEALE, S. J. 1974. Possible histories of the obliquity of Mercury. *Astron J.* **79,** 722–744.

PEALE, S. J. 1977. Rotational histories of the natural satellites. In *Planetary Satellites* (J. A. Burns, Ed.), pp. 87–112. Univ. of Arizona Press, Tucson.

PEALE, S. J., AND P. CASSEN 1978. Contribution of tidal dissipation to lunar thermal history. *Icarus* **36,** 245–269.

PEALE, S. J., P. CASSEN, AND R. T. REYNOLDS 1979. Melting of Io by tidal dissipation. *Science* **203,** 892–894.

PROCTOR, T. M. 1966. Low-temperature speed of

sound in single-crystal ice. *J. Acoust. Soc. Amer.* **39,** 972–977.

TYLER, G. L., D. N. SWEETNAM, J. D. ANDERSON, J. K. CAMPBELL, V. R. ESHLEMAN, D. P. HINSON, G. S. LEVY, G. F. LINDAL, E. A. MAROUF, AND R. A. SIMPSON 1986. Voyager 2 radio science observations of the Uranian system: Atmosphere, rings, and satellites. *Science* **233,** 79–84.

WARD, W. R. 1975a. Past orientation of the lunar spin axis. *Science* **189,** 377–379.

WARD, W. R. 1975b. Tidal friction and generalized Cassini's laws in the Solar System. *Astron. J.* **80,** 64–70.

WISDOM, J. 1987. Rotational dynamics of irregularly shaped natural satellites. *Astron. J.* **94,** 1350–1360.